Original Article

Contrast-enhanced pelvic magnetic resonance imaging (MRI) for the prediction of treatment response in mucinous rectal cancer

Maria El Homsi[1]^, Onur Yildirim[1], Natalie Gangai[1], Jinru Shia[2], Marc J. Gollub[1], Yousef Mazaheri[1,3]

[1]Department of Radiology, Memorial Sloan Kettering Cancer Center, New York, NY, USA; [2]Department of Pathology, Memorial Sloan Kettering Cancer Center, New York, NY, USA; [3]Department of Medical Physics, Memorial Sloan Kettering Cancer Center, New York, NY, USA

Contributions: (I) Conception and Design: M El Homsi, M Gollub, Y Mazaheri; (II) Administrative support: N Gangai; (III) Provision of study materials or patients: M El Homsi, M Gollub, Y Mazaheri, J Shia; (IV) Collection and assembly of data: M EL Homsi, O Yildirim; (V) Data analysis and interpretation: M El Homsi, M Gollub, Y Mazaheri; (VI) Manuscript writing: All authors; (VII) Final approval of manuscript: All authors.

Correspondence to: Maria El Homsi, MD. Department of Radiology, Memorial Sloan Kettering Cancer Center, 1275 York Avenue, New York, NY, USA. Email: elhomsim@mskcc.org.

Background: In mucinous rectal cancer, it can be difficult to differentiate between cellular and acellular mucin. The purpose of this study was to evaluate, in patients with mucinous rectal cancer, the value of static enhancement (enh) and pharmacokinetic parameters of dynamic contrast-enhanced (DCE) magnetic resonance imaging (MRI) in predicting pathologic complete response.

Methods: This retrospective cross-sectional study performed at Memorial Sloan Kettering Cancer Center included 43 patients (24 males and 19 females; mean age, 57 years) with mucinous rectal cancer who underwent MRI at baseline as well as after neoadjuvant chemoradiotherapy but before surgical resection between 2008 and 2019. Two radiologists independently segmented tumors on contrast-enhanced axial 3D T1-weighted images and sagittal DCE magnetic resonance images. On contrast-enhanced axial T1-weighted images, the static parameters enh and relative enhancement (renh) were estimated. On DCE images, the pharmacokinetic parameters K^{trans}, k_{ep}, relative K^{trans} (rK^{trans}), and relative k_{ep} (rk_{ep}) were estimated. Associations between all parameters with pathologic complete response were tested using Wilcoxon signed-rank tests. Receiver operating characteristic (ROC) analysis was performed to assess the area under the curve (AUC) for each parameter.

Results: Of the 43 patients who were included in the study, 42/43 (98%) had evaluable contrast-enhanced axial T1-weighted images and 35/43 (81%) had evaluable DCE images. Of the patients with evaluable contrast-enhanced axial T1-weighted images, 9/42 (21%) had pathologic complete response and 33/42 (79%) did not have pathologic complete response. For reader 1, enh(pre-neoadjuvant chemotherapy), enh(post-neoadjuvant chemotherapy), and renh were significant predictors of pathologic complete response [P=0.045 (AUC =0.73), 0.039 (AUC =0.74), and 0.0042, respectively]. For reader 2, enh(pre-neoadjuvant chemotherapy) and renh were significant predictors [P=0.021 (AUC =0.77) and 0.002, respectively]. For renh, the AUC was 0.83 for reader 1, and 0.82 for reader 2. Meanwhile, of those patients with evaluable DCE images, 9/35 (26%) had pathologic complete response and 26/35 (74%) did not have pathologic complete response. K^{trans}(pre-neoadjuvant chemotherapy), k_{ep}(pre-neoadjuvant chemotherapy), and rk_{ep} were significant predictors [P=0.016 (AUC =0.73), 0.00057 (AUC =0.81), and 0.0096 (AUC =0.74), respectively].

Conclusions: Static and pharmacokinetic parameters of contrast-enhanced MRI show promise to predict neoadjuvant treatment response. Static enh parameters, which are simpler to assess, showed the strongest prediction.

^ ORCID: 0000-0002-8483-3653.

Keywords: Mucinous rectal cancer; contrast-enhanced magnetic resonance imaging (contrast-enhanced MRI); pathologic complete response

Submitted Oct 19, 2023. Accepted for publication Mar 26, 2024. Published online May 24, 2024.
doi: 10.21037/qims-23-1463
View this article at: https://dx.doi.org/10.21037/qims-23-1463

Introduction

Mucinous cancer is a rare type of cancer defined by the World Health Organization as greater than 50% tumor composition by extracellular mucin (1). Among colorectal tumors, mucinous rectal cancer commonly affects the right colon and accounts for approximately 10% of all rectal tumors (2). Compared to its non-mucinous counterpart, mucinous rectal cancer is generally associated with a higher T category at diagnosis (3), increased risk of metastases (4), higher local recurrence and venous invasion rates (5), and worse survival (6). Thus, a reliable imaging tool to predict pathological complete response (pCR) in mucinous rectal cancer following preoperative neoadjuvant chemoradiation therapy (CRT) could be very valuable.

To date, because of the T2-weighted hyperintense signal of mucin, magnetic resonance imaging (MRI) has an accuracy of 96–97% for detecting the mucinous histologic type of rectal cancer, with a sensitivity of 94–100% and a specificity of 95–98% (4,5,7), as well as excellent interobserver agreement (8). Mucinous rectal cancers show less restricted diffusion and less contrast enhancement (enh) compared to non-mucinous cancers (8). However, it is difficult to distinguish between cellular mucin (residual tumor considered to be present) and acellular mucin (tumor considered eradicated) on T2-weighted imaging (9), albeit the cellular component is reportedly more heterogeneous and shows intermediate signal intensity (SI) (10). Moreover, post neoadjuvant chemoradiation therapy (nCRT), mucin may persist or arise *de novo* as a form of non-mucinous tumor response, and it can be difficult to differentiate between cellular and acellular mucin since both may appear T2 hyperintense.

Dynamic contrast-enhanced (DCE)-MRI is an imaging technique that can provide quantitative pharmacokinetic parameters and has been shown to be clinically useful in quantifying tumor vasculature and tumor perfusion in many organs (11). Following intravenous injection of a contrast agent, sequential images are acquired while the contrast agent passes through the tissue of interest. The model proposed by Toft's is considered the standard model for the analysis of DCE-MRI and is readily used to estimate pharmacokinetic parameters, including K^{trans}, which is an estimate of the influx forward volume transfer constant between the blood plasma and the extravascular, extra-cellular space (EES), and k_{ep}, which is an estimate of the rate constant between the EES and the blood plasma (12). In non-mucinous rectal cancer, several studies have assessed the role of DCE-MRI in predicting pCR (13-15) and in downstaging tumors (16-18); however, only a single study has assessed the role of quantitative DCE-MRI for downstaging mucinous and non-mucinous rectal cancer after nCRT, demonstrating that a lower amplitude, where amplitude characterizes the relative interstitial space volume into which the contrast medium diffuses through capillaries (19), is associated with better response to treatment (20). We postulated that in the challenging mucinous subtype of rectal cancer, gadolinium-based contrast-enhanced rectal MRI acquired pre- and post-nCRT can be used to predict tumor response by using both static contrast-enhanced data as well as pharmacokinetic data. As an alternative to quantitative DCE pharmacokinetic data modeling, simple percentage enh of the gadolinium-based contrast agent can be measured on static images to generate a measure of contrast enh when only static pre- and post-contrast data are available. This static-based approach does not rely on data modeling but is sensitive to experimental factors such as hardware, sequence parameters, and contrast dose.

To the best of our knowledge, DCE-MRI has not been used to detect pCR in patients with mucinous rectal cancer. Prior studies using DCE-MRI have focused primarily on non-mucinous rectal cancer (13-18). On the other hand, a study using a linear open two-compartment model function (commonly referred to as Brix model) found that the contrast medium exchange rate (k_{21}) is significantly higher in non-mucinous tumors as compared to mucinous tumors at pre-treatment MRI. This study also found that chemoradiation affects pharmacokinetic parameters greater in non-mucinous tumors as compared to the mucinous

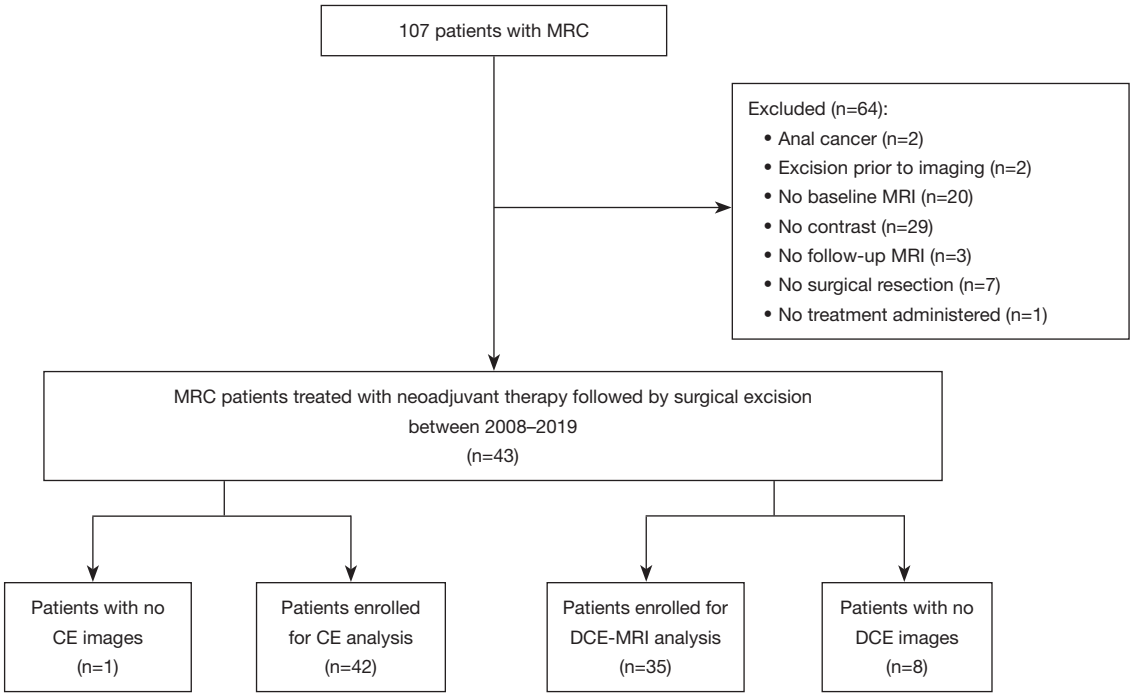

Figure 1 Flowchart showing the number of patients included in the study. MRC, mucinous rectal cancer; MRI, magnetic resonance imaging; CE, contrast-enhanced; DCE-MRI, dynamic contrast-enhanced magnetic resonance imaging; DCE, dynamic contrast-enhanced.

subtype (20). However, no study has assessed the role of static contrast-enhanced MRI data in mucinous rectal cancer. Thus, the purpose of this study was to evaluate, in patients with mucinous rectal cancer, the role of static enh and pharmacokinetic parameters of contrast-enhanced MRI in identifying patients with pCR. We present this article in accordance with the STROBE reporting checklist (available at https://qims.amegroups.com/article/view/10.21037/qims-23-1463/rc).

Methods

Study population

This retrospective study was compliant with the Health Insurance Portability and Accountability Act and was approved by the institutional review board of Memorial Sloan Kettering Cancer Center (IRB No. 18-136), individual consent for this retrospective analysis was waived. The study was conducted in accordance with the Declaration of Helsinki (as revised in 2013). A total of 107 consecutive patients with mucinous rectal cancer treated with neoadjuvant therapy between 2008 and 2019 were identified. The exclusion criteria were: (I) absence of contrast-enhanced MRI of the rectum for staging and restaging, and/or (II) no surgical resection. Of 107 patients, 64 patients were excluded, yielding a final study sample of 43 patients (24 males, 19 females; mean age, 57 years). Across the entire study sample, contrast-enhanced 3D T1-weighted imaging (static imaging) was available for analysis for 42 patients, while DCE imaging was available for analysis for 35 patients. One of these 35 patients did not have static imaging but had only DCE images. Seven patients were excluded from DCE imaging analysis as their images were deemed non-diagnostic primarily due to patient and/or bowel motion. A summary flowchart of patient inclusion into the study is presented in *Figure 1*.

The average time between the end of nCRT and surgery was 149±108 days. Patients were treated with nCRT consisting of 5-fluorouracil-oxaliplatin (FOLFOX) or Xeloda combined with radiation therapy (4,500 cGy). The type of nCRT administered to 5 patients was not available.

MRI protocol

All 43 patients had two MRI exams performed, one baseline exam before nCRT and the other after nCRT but before

Table 1 Sequence parameters for static contrast-enhanced T1-weighted imaging and DCE-MRI acquisition at 1.5 and 3 T

Sequence parameter	1.5 T		3 T	
	Static T1WI	DCE-MRI	Static T1WI	DCE-MRI
TR, ms	3.92	3.2	3.6–5.4	3.4
TE, ms	1.9	1.25	1.46	1.16
Flip angle	15°	12°	15°	12°
Slice thickness (mm)	3	5	3	4
Matrix	320×192	256×128	288×224	256×224
FOV, mm^2	28–36	24	28–36	24

DCE-MRI, dynamic contrast-enhanced magnetic resonance imaging; T1WI, T1-weighted imaging; TR, repetition time; TE, echo time; FOV, field of view.

surgery. All MRI exams were performed using either a 1.5 T unit (n=30 MRIs) or a 3 T unit [n=56 MRIs (both Signa HDX; GE Healthcare, Chicago, IL, USA]. For signal reception, a pelvic eight-channel phased-array coil was used. At both field strengths, the standard exam included a fat-suppressed spoiled gradient-echo T1-weighted sequence to obtain static images before and after intravenous injection of the gadolinium-based contrast agent (Gd-DTPA; Magnevist, Bayer Schering, Germany). The contrast agent was administered at 0.1 mL/kg body weight (0.1 mmol/kg) as a bolus at a flow rate of approximately 2 mL/s and was injected after 1 minute of starting data acquisition. The temporal resolution ranged from 6–9 s. In addition, DCE images were obtained using a Differential Subsampling with Cartesian Ordering (DISCO) sequence (21). Both contrast-enhanced T1-weighted and DCE images were obtained within 3 minutes after intravenous gadolinium injection to standardize the timing of acquisition. The 1.5 and 3 T contrast-enhanced T1-weighted and DCE imaging parameters are summarized in *Table 1*. Other sequences included axial, coronal, and sagittal T2-weighted fast spin-echo sequences [repetition time (TR)/effective echo time (TE) =4,000/102 ms, echo train length =15, slice thickness =4 mm, inter-slice gaP =1 mm, field of view (FOV) =18–24 cm, acquisition matrix =320×224], and axial diffusion-weighted imaging (TR/TE =6,000/66.6 ms, section thickness =5 mm, no inter-slice gap, FOV =16 cm, acquisition matrix =128×128, b-values =0, 400, 800, and 1,500 s/mm^2). Parallel imaging with a factor of 2 and fat suppression was also used.

MRI evaluation

The acquired imaging datasets were transferred to a personal computer, and imaging evaluation was performed with in-house software. Two radiologists independently segmented all tumor areas, drawing free-form regions of interest (ROIs) on the contrast-enhanced T1-weighted static images and DCE images. Specifically, using ImageJ software (version 1.80, National Institutes of Health, Bethesda, MD, USA), one radiologist (M.E.H. with 2 years of experience; reader 1), blinded to histopathological results, manually segmented tumors on the static axial T1-weighted images as well as the sagittal DCE images, using sagittal T2-weighted images as a reference for tumor location (*Figure 2*). A second radiologist (O.Y. with 1 year of experience; reader 2) manually segmented tumors on only the static axial T1-weighted images. A senior radiologist (M.J.G. with 20 years of experience) was consulted throughout the analysis but this radiologist did not perform any image segmentation for the study.

For all ROIs, parametric maps of pharmacokinetic coefficients were generated using mean SI curves in the ROIs; a MATLAB program (version R2014b, The MathWorks, Inc., Natick, MA, USA) was employed for this purpose. From the static axial T1-weighted images, enh values were estimated and expressed as means ± standard deviation (SDs). From the DCE images, the pharmacokinetic parameters K^{trans} and k_{ep} were estimated and also expressed as means ± SDs. First, mean SI curves were extracted and converted to dynamic longitudinal relaxation rate. The measured signal, $S(t)$, can be converted into tissue contrast concentration time curves, $C_t(t)$, using the following formula (22):

$$C_t(t) \approx \frac{1}{T_{10} r_1} \cdot \frac{S(t) - S(0)}{S(0)} \quad [1]$$

where T_{10} is the pre-enh relaxation time, $S(0)$ is the pre-contrast signal, and r_1 is the relaxivity of the contrast

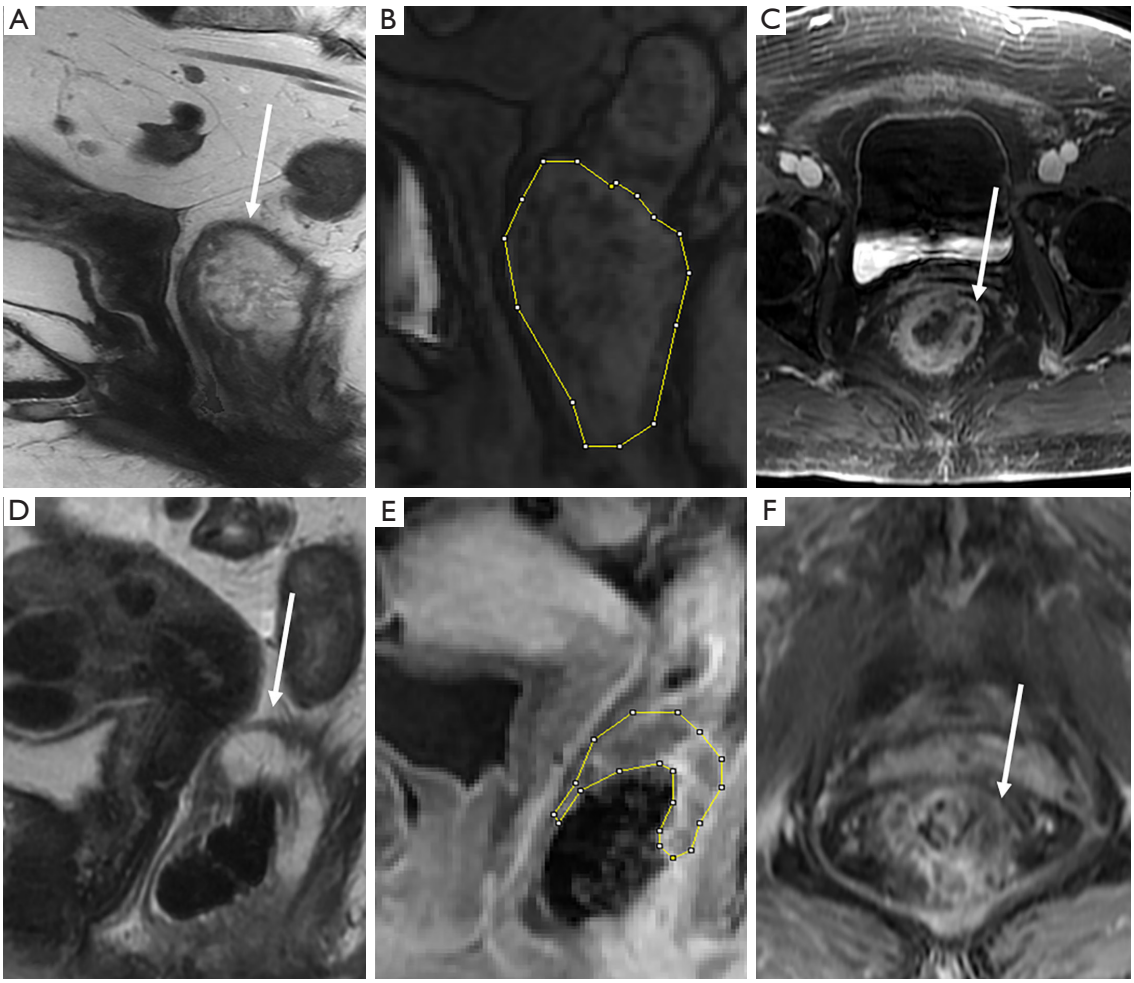

Figure 2 A 73-year-old woman with mucinous rectal cancer. Baseline, pre-neoadjuvant chemoradiation therapy MRI (A) sagittal T2-weighted image; (B) sagittal T1-weighted image, and (C) contrast-enhanced axial 3D T1-weighted image show a mid-rectal mucinous tumor (arrows). Post neoadjuvant chemoradiation therapy (D) sagittal T2-weighted image, (E) sagittal T1-weighted image, and (F) contrast-enhanced axial 3D T1-weighted image show decreased tumor size (arrows) with persistent mucinous component demonstrating heterogenous enhancement. Pathology showed 60% treatment response. MRI, magnetic resonance imaging; 3D, three-dimensional.

agent, assumed to be a constant (4.5 $s^{-1}mM^{-1}$) (23). Our study did not include quantitative T_{10} measurements; rather, a literature-based value for T_{10} in mucinous tumors, 1,986.1±163.3 ms, was used (24). In Toft's analysis of DCE imaging, an estimate of the arterial input function (AIF) is required. For our study, we used the Parker-based population-averaged AIF (25). K^{trans} and mean k_{ep} were estimated by fitting the DCE data to the Toft's perfusion model with a population-based AIF (12).

In addition to deriving these contrast-enhanced parameters from both the pre-nCRT MRIs and the post-nCRT MRIs, the relative changes of all these parameters between the pre- and post-nCRT MRIs were also derived. For example, relative K^{trans} and relative k_{ep} were calculated as the relative percentage differences in Toft's pharmacokinetic parameters between the pre- and post-nCRT MRIs. Representative images, including contrast-enhanced static axial T1-weighted images, DCE parametric maps, and corresponding DCE curves, in a pCR patient and non-pCR patient are shown in *Figures 3,4*, respectively.

Histopathologic evaluation

The reference standard was the histopathologic report

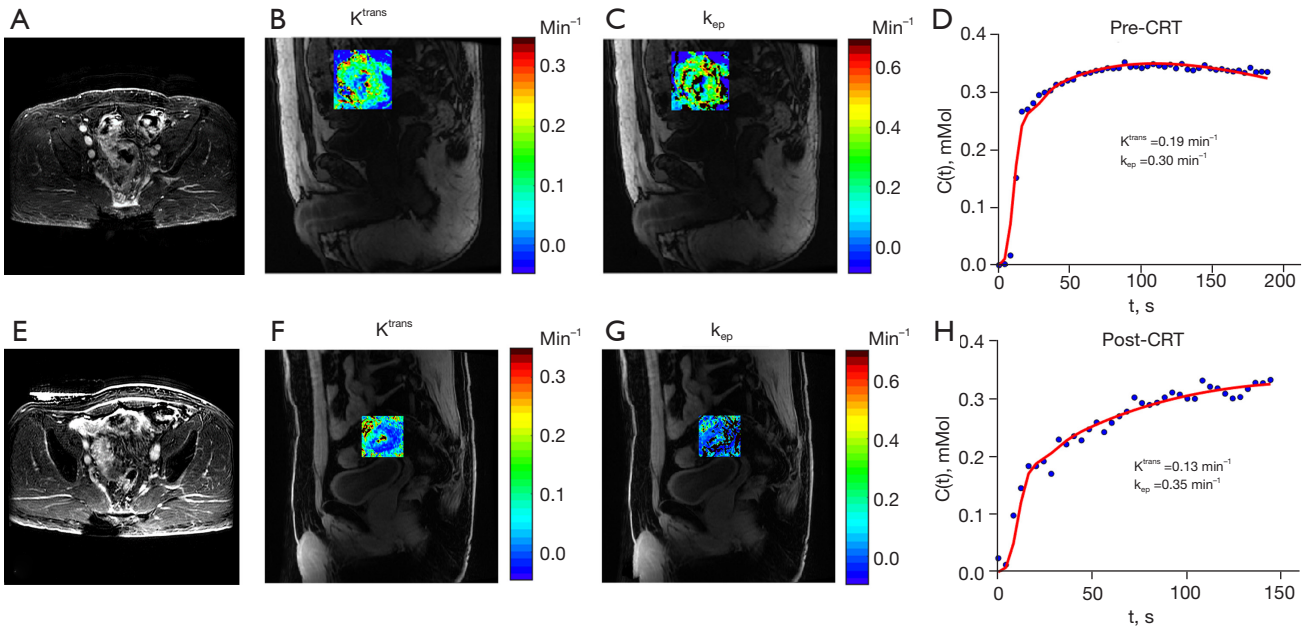

Figure 3 MR images of a 61-year-old man with mucinous rectal cancer who achieved pathologic complete response. Baseline, pre-neoadjuvant chemoradiation therapy MRI: (A) contrast-enhanced axial T1-weighted image delineating the tumor. (B,C) Color-coded K^{trans} and k_{ep} maps show a dominant green color in the corresponding tumor with K^{trans} 0.19 min^{-1} and k_{ep} 0.30 min^{-1}. (D) Curves of both K^{trans} and k_{ep}. Post-neoadjuvant chemoradiation therapy MRI: (E) contrast-enhanced axial T1-weighted image delineating residual tumor. (F,G) Color-coded K^{trans} and k_{ep} maps show a dominant blue color in the corresponding tumor with K^{trans} 0.13 min^{-1} and k_{ep} 0.35 min^{-1}. (H) Curves of both K^{trans} and k_{ep}. K^{trans}, influx forward volume transfer constant between the blood plasma and the extravascular extra-cellular space; k_{ep}, rate constant between the extravascular extra-cellular space and the blood plasma; CRT, chemoradiation therapy; MR, magnetic resonance; MRI, magnetic resonance imaging.

of the surgical resection specimens. We performed a retrospective chart review of pathologic results, and no additional pathologic analysis was done solely for our project. At our institution, all histopathologic analyses are performed by specialized gastrointestinal pathologists who report their findings as response rates (26).

Statistical analysis

Quantitative results were presented as means ± SDs. Differences in contrast-enhanced static T1-weighted imaging and DCE parameter values between pCR and non-pCR were tested for statistical significance using Wilcoxon signed-rank tests. Intraclass correlation coefficient (ICC) was estimated to evaluate the agreement between the two readers. Two-sided test P values less than 0.05 were considered to indicate a statistically significant difference. In addition, receiver operating characteristic (ROC) analysis was performed to assess the diagnostic performance, assessed in terms of the area under the curve (AUC), for each contrast-enhanced static T1-weighted imaging and DCE parameter. All statistical analyses were performed using MATLAB software.

Results

Patient characteristics

The mean time interval between the two MRIs (obtained before chemoradiotherapy and before surgery) was 247± 167 days. Among the patients with evaluable DCE images, 9/35 (26%) achieved pCR and 26/35 (74%) did not achieve pCR. Among the patients with evaluable static contrast-enhanced T1-weighted images, 8/42 (19%) achieved pCR and 34/42 (81%) did not achieve pCR. Surgical resection consisted of low anterior resection (n=18) and abdominoperineal resection (n=24). Patient and tumor characteristics are summarized in *Table 2*.

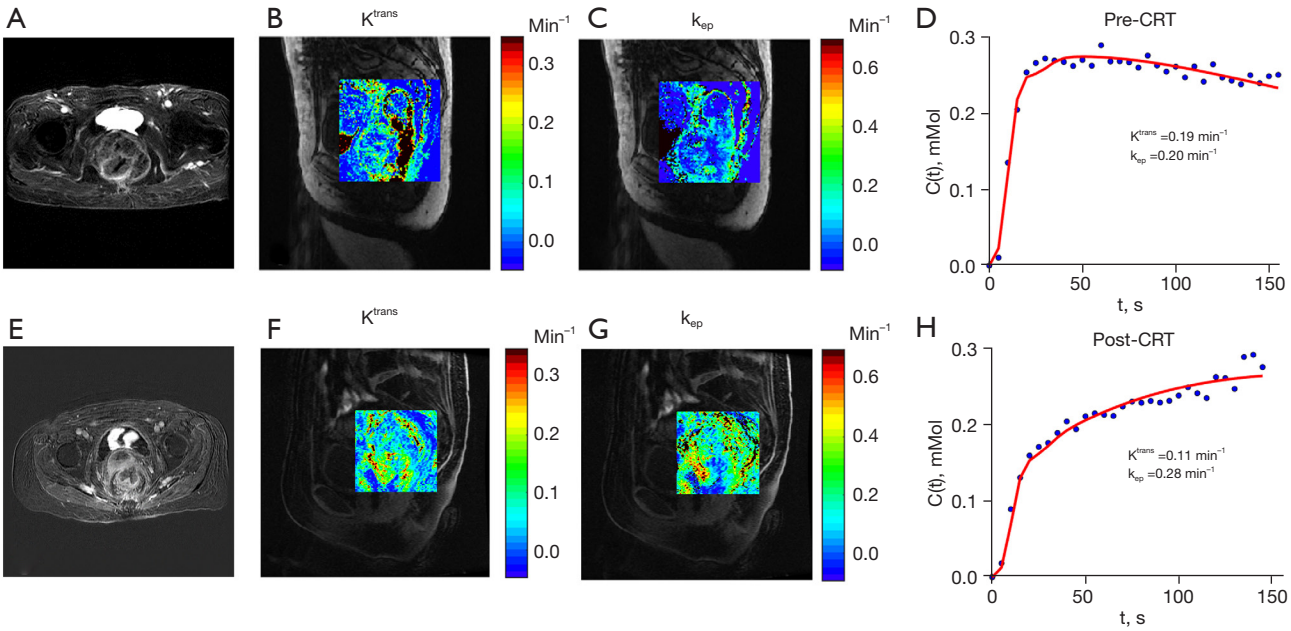

Figure 4 MR images of an 82-year-old woman with mucinous rectal cancer who achieved 20% treatment response after chemoradiation therapy. Baseline, pre-neoadjuvant chemoradiation therapy MRI: (A) contrast-enhanced axial T1-weighted image delineating the tumor. (B,C) Color-coded K^{trans} and k_{ep} maps show a mixture of blue and green colors in the corresponding tumor with K^{trans} 0.19 min^{-1} and k_{ep} 0.20 min^{-1}. (D) Curves of both K^{trans} and k_{ep}. Post-neoadjuvant chemoradiation therapy MRI: (E) contrast-enhanced axial T1-weighted image delineating residual tumor. (F,G) Color-coded K^{trans} and k_{ep} maps show increased green color in the corresponding tumor with K^{trans} 0.11 min^{-1} and k_{ep} 0.28 min^{-1}. (H) Curves of both K^{trans} and k_{ep}. K^{trans}, influx forward volume transfer constant between the blood plasma and the extravascular extra-cellular space; k_{ep}, rate constant between the extravascular extra-cellular space and the blood plasma; CRT, chemoradiation therapy; MR, magnetic resonance; MRI, magnetic resonance imaging.

Comparison between pCR and non-pCR groups

Static T1-weighted imaging parameters of enh and relative enhancement (renh)

Enh and renh values at pre- and post-nCRT MRI as assessed by the two readers are given in *Table 3*. *Figure 5* also shows the box-and-whisker plots of enh and renh values for the group of patients who achieved pCR (i.e., pCR group) and the group of patients that did not achieve pCR (i.e., non-pCR group).

For reader 1, at pre-nCRT MRI, the enh of 1.77±0.27 in the pCR group was significantly higher than the enh of 1.5±0.80 in the non-pCR group (P=0.045); enh yielded an AUC of 0.73. On the other hand, at post-nCRT MRI, the enh of 1.12±0.43 in the pCR group was significantly lower than the enh of 1.60±0.65 in the non-pCR group (P=0.039); enh yielded an AUC of 0.74.

Likewise, for reader 2, at pre-nCRT MRI, the enh of 1.71±0.34 in the pCR group was significantly higher than the enh of 1.34±0.69 in the non-pCR group (P=0.021); enh yielded an AUC of 0.77. At post-nCRT MRI, however, while the enh of 1.11±0.44 in the pCR group was lower than the enh of 1.43±0.57 in the non-pCR group, this difference was not significant.

For both readers, renh was significantly different between the pCR and non-PCR groups (P=0.0042 and 0.002 for reader 1 and reader 2, respectively). Renh yielded AUCs of 0.83 and 0.82, respectively, for reader 1 and reader 2.

The level of agreement on enh and renh of the tumor on static contrast-enhanced T1-weighted imaging between readers 1 and 2 is summarized in *Table 4*. Across all patients, there was high agreement for enh(pre-nCRT) (ICC =0.88) and enh(post-nCRT) (ICC =0.82) measurements, but low agreement for renh measurements (ICC =0.24).

DCE pharmacokinetic parameters of K^{trans}, k_{ep}, relative K_{trans}, and relative k_{ep}

Values for each DCE pharmacokinetic parameter at pre-

and post-CRT MRI are given in *Table 5*; the values of these parameters are also reflected in box-and-whisker plots in *Figure 5*.

At pre-nCRT MRI, the K^{trans} of 0.21±0.073 min^{-1} in the pCR group was higher than the K^{trans} 0.16±0.072 min^{-1} in the non-pCR group, with the difference being significant (P=0.016); K^{trans} yielded an AUC of 0.73. Meanwhile, also at pre-nCRT, the k_{ep} of 0.20±0.10 min^{-1} was significantly lower than the k_{ep} of 0.33±0.10 min^{-1} in the non-pCR group (P=0.00057); k_{ep} yielded an AUC of 0.81.

At post-nCRT MRI, differences in K^{trans} and k_{ep} between the pCR and non-pCR groups were not significant (P=0.27 and 0.48, respectively).

The relative K^{trans} was not significantly different between the pCR and non-pCR groups (P=0.11). However, the relative k_{ep} was significantly different between the pCR and non-PCR groups (P=0.0096); relative k_{ep} yielded an AUC of 0.74.

Table 2 Patient and tumor characteristics

Characteristic	Value (n=43)
Mean age (years)	57
Biological sex, n (%)	
Female	19 (44)
Male	24 (56)
T stage, n (%)	
T1/2	2 (4.7)
T3a	2 (4.7)
T3b	11 (25.6)
T3c	7 (16.3)
T3d	4 (9.3)
T4a	2 (4.7)
T4b	15 (34.7)
Location from the anal verge, n (%)	
Low (0–5 cm)	24 (55.8)
Mid (5.1–10 cm)	10 (23.3)
High (10.1–15 cm)	9 (20.9)
Mucin content, n (%)	
≤50%	28 (65.1)
>50%	15 (34.9)
Size, n (%)	
≤5 cm	10 (23.3)
>5 cm	33 (76.7)

Discussion

In this study, we investigated the role of contrast-enhanced MRI parameters (both static T1-weighted imaging parameters and DCE pharmacokinetic parameters) at pre- and post-nCRT MRI to predict pCR in patients with mucinous rectal cancer. The static parameters of enh at both pre- and post-nCRT MRI and of renh were significantly predictive of pCR for reader 1, with AUCs from 0.73–0.86; meanwhile, the mean enh on pre-nCRT MRI only and the renh were statistically predictive of pCR for reader 2, with AUCs from 0.77–0.82. We demonstrated that DCE pharmacokinetic parameters can also help to predict pCR by using K^{trans} and k_{ep} at pre-nCRT MRI and relative k_{ep}, with AUCs of 0.71, 0.81, and 0.84, respectively. K^{trans} and k_{ep} at pre-nCRT MRI were higher in the pCR group compared to the non-pCR group.

We interpret these results to indicate that like non-mucinous tumors, nCRT effects include the obliteration of tumor vasculature and progressive hypo-enh even in mucinous tumors whose solid components are not so evident. While we did not compare mucinous and non-mucinous tumors in this

Table 3 Enhancement and relative enhancement of the tumor on static contrast-enhanced T1-weighted imaging as assessed by readers 1 and 2

Parameter	pCR		Non-pCR		P value	
	Reader 1	Reader 2	Reader 1	Reader 2	Reader 1	Reader 2
Enh(pre-nCRT)	1.77±0.27	1.71±0.34	1.5±0.80	1.34±0.69	0.045	0.021
Enh(post-nCRT)	1.12±0.43	1.11±0.44	1.60±0.65	1.43±0.57	0.039	0.21
Renh	0.31±0.77	0.22±0.59	–0.37±0.22	–0.35±0.23	0.0042	0.002

Values are expressed as mean ± standard deviation. pCR, pathologic complete response; enh, enhancement; nCRT, neoadjuvant chemoradiation therapy; Renh, relative enhancement.

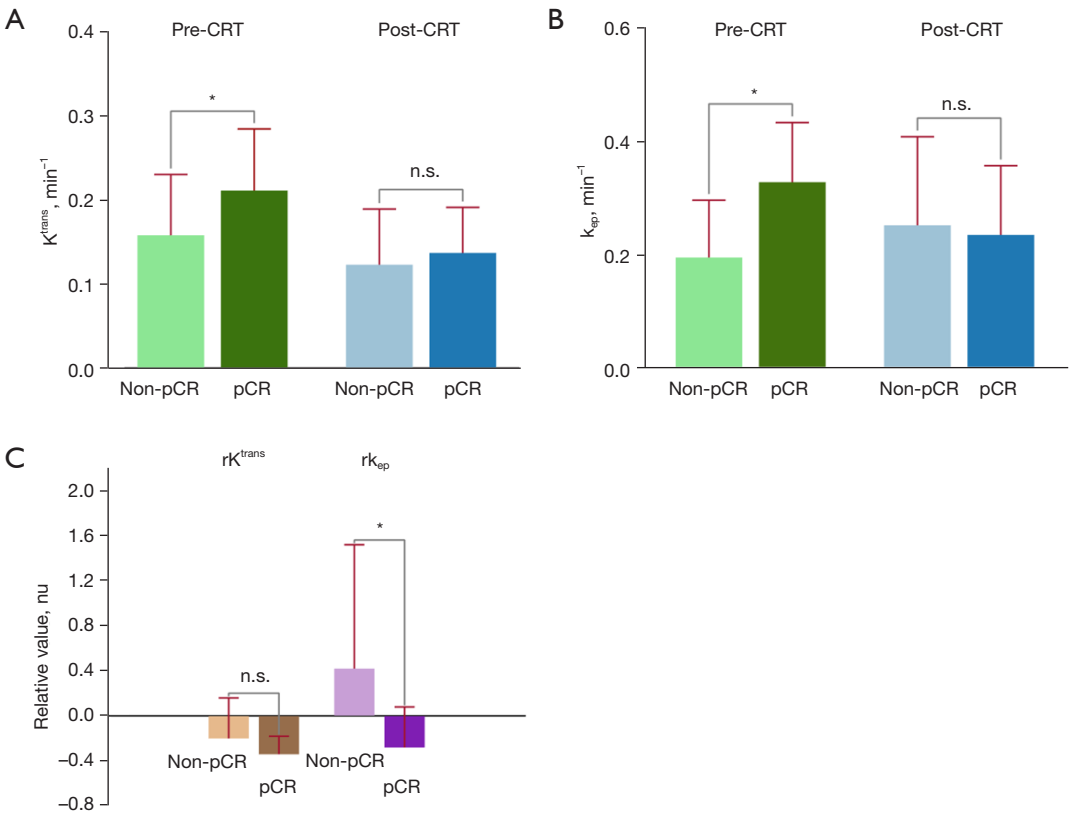

Figure 5 Box-and-whisker plots of parametric maps derived from DCE acquisition for (A) K^{trans}, (B) k_{ep}, and (C) relative K^{trans}, and relative k_{ep}. On each box, the central mark indicates the median parameter value, and the bottom and top edges of the box indicate the 25th and 75th percentiles, respectively. * indicates statistical significance. n.s. indicates no statistical significance; relative K^{trans} and relative k_{ep} were calculated as the relative percentage differences in Toft's pharmacokinetic parameters between the pre- and post-nCRT MRIs. CRT, chemoradiation therapy; pCR, pathologic complete response; K^{trans}, influx forward volume transfer constant between the blood plasma and the extravascular extra-cellular space; k_{ep}, rate constant between the extravascular extra-cellular space and the blood plasma; rK^{trans}, relative K^{trans}; rk_{ep}, relative k_{ep}; nu, no unit; DCE, dynamic contrast enhanced; nCRT, neoadjuvant chemoradiation therapy; MRI, magnetic resonance imaging.

Table 4 Agreement on enhancement and relative enhancement of the tumor on static contrast-enhanced T1-weighted imaging between readers 1 and 2

Parameter	ICC	95% CI	
		Lower	Upper
Enh(pre-nCRT)	0.88	0.78	0.93
Enh(post-nCRT)	0.82	0.68	0.90
Renh	0.24	0.13	0.51

ICC, intraclass correlation coefficient; CI, confidence interval; enh, enhancement; nCRT, neoadjuvant chemoradiation therapy; Renh, relative enhancement.

study, these results confirm what is known about the expected effects of chemoradiation (27) and that mucinous tumors respond as expected at the microenvironment level. The greater accuracy and significance of static parameters are encouraging since static parameters are simpler to use.

The lack of significance of post-nCRT K^{trans} as well as relative K^{trans} parameters that are usually most illuminating in other rectal cancer studies is puzzling and would require further study. Meanwhile, the pharmacokinetic parameters pre-nCRT K^{trans} and k_{ep} showed value to predict pCR for both readers. Our results support the hypothesis by Tong

Table 5 Pre- and post-neoadjuvant chemoradiation therapy K^{trans}, k_{ep}, relative K^{trans}, and relative k_{ep}

Parameter	pCR	Non-pCR	P value
K^{trans}(pre-nCRT) (min^{-1})	0.21±0.073	0.16±0.072	0.016
k_{ep}(pre-nCRT) (min^{-1})	0.20±0.10	0.33±0.10	0.00057
K^{trans}(post-nCRT) (min^{-1})	0.14±0.054	0.12±0.067	0.27
k_{ep}(post-nCRT) (min^{-1})	0.24±0.12	0.25±0.16	0.48
rK^{trans}	−0.34±0.16	−0.20±0.36	0.11
rk_{ep}	−0.28±0.36	0.42±1.10	0.0096

Values are expressed as means ± standard deviations. K^{trans}, influx forward volume transfer constant between the blood plasma and the extravascular extra-cellular space; k_{ep}, rate constant between the extravascular extra-cellular space and the blood plasma; pCR, pathologic complete response; nCRT, neoadjuvant chemoradiation therapy; rK^{trans}, relative K^{trans}; rk_{ep}, relative k_{ep}.

et al. (13) that tumors with more permeable vasculature would be more responsive to chemotherapy, due to the greater combined permeability and flow, as captured by K^{trans}; similarly, these tumors would have a higher return blood flow from the tumor to the endothelial system, as captured by k_{ep}. Therefore, the high pre-nCRT K^{trans} in our study indicates better blood flow, hence increased oxygenation to the tumor, and hence increased radiosensitivity and better delivery of chemotherapy (27). These findings are encouraging and further validation of these biophysical models and associated hypotheses would be valuable.

To date, studies in rectal cancer have largely focused on non-mucinous rectal cancer rather than mucinous rectal cancer. Prior studies to predict pCR in non-mucinous rectal cancer using DCE pharmacokinetic parameters have yielded conflicting results. Tong *et al.* (13) showed that pre-CRT K^{trans} and k_{ep} were higher in the pCR group compared to the non-pCR group and were predictive of pCR, with AUCs of 0.92 and 0.67, respectively, while post-CRT K^{trans} and k_{ep} were not predictive of pCR, similar to our results. On the other hand, in studies by Gollub *et al.* and Kim *et al.* (15,16), K^{trans} did not have a significant role in the baseline prediction of pCR in non-mucinous rectal cancer, albeit having a significant role in the prediction of good responder rectal cancers to therapy. Meanwhile, Intven *et al.* (14) demonstrated that post-CRT K^{trans} and rK^{trans} were predictive of pCR in non-mucinous rectal cancer, with AUCs ranging from 0.75–0.89; however, pre-CRT K^{trans} had no significant predictive role in 51 patients with only 11.8% with pCR. A systematic review by Dijkhoff *et al.* (28) found that the most commonly reported significant pre-CRT predictor of pCR in rectal cancer was K^{trans}, whereby a high K^{trans} value of 0.36 min^{-1} was predictive of good or complete response across four studies, albeit the range of the reported pre-CRT K^{trans} values ranged considerably from 0.17–0.42. Meanwhile, among post-CRT DCE parameters, Dijikhoff *et al.* found that a reduction of about a third (32–36%) in K^{trans} values was predictive of good or complete response across several studies, and a lower post-CRT K^{trans} value was predictive of good or complete response across two studies. Only a single study has assessed the role of DCE in mucinous rectal cancer, wherein no patients achieved pCR (20). This study showed that a lower amplitude of contrast between the capillaries and interstitial space of the tumor, which represents a smaller interstitial space, was predictive of downstaging post therapy. To our best knowledge, no prior study has investigated the prediction of tumor response in mucinous rectal cancer using static T1-weighted imaging parameters. The discrepancies and gaps in the literature to date, along with the findings this study, show the need of larger studies to implement DCE and other MRI parameters (e.g., static T1-weighted imaging parameters) for the prediction of pCR.

In this study, the role of T1-weighted imaging parameters for the prediction of pCR was shown to be promising. For both readers, enh at pre-nCRT MRI and renh were significant to predict pCR, with AUCs ranging from 0.73–0.86. Enh at post-nCRT MRI was only significant for reader 1 with an AUC of 0.74. The difference between the two readers can be explained by the different level of experience between them and the challenge in segmenting rectal tumors post nCRT, and hence the need for automated segmentation methods. Overall, however, the static contrast enh analysis method has not been used before in assessing treatment response in rectal cancer and can be an easy and

accessible way compared to DCE analysis to predict pCR.

Regarding the clinical implications of our study, our results indicate that gadolinium-based contrast agent administration yields similar results in mucinous and non-mucinous tumors. Regardless of whether a tumor is mucinous or non-mucinous, a better perfused (i.e., less hypoxic) tumor will be able to receive more chemotherapy and respond better to radiotherapy. Post-nCRT enh for reader 1 was higher in the non-pCR group, suggesting more contrast retention, possibly in the tumor stroma. Furthermore, relative k_{ep} differed between pCR and non-pCR patients, indicating differences in contrast retention/outflow in the tumors of these patients. These findings suggest the need for further investigation regarding the ability of DCE parameters to differentiate cellular and acellular mucin using gadolinium-contrast-enhanced MRI. Indeed, in the assessment of mucinous treatment response, several imaging factors, including imaging parameters that can distinguish between cellular and acellular mucin, will have an important role.

The present study had some limitations. First, the retrospective nature of our study may have resulted in a selection bias of the patients. Second, the number of cases was small, with the pCR group consisting of only 9 cases, but this reflected a typically representative fraction of patients with respect to pCR. Third, DCE-MRI is sensitive to motion artifacts, specifically those from rectal and colonic peristalsis. Fourth, as the data were acquired using different field strengths across a wide time period, there was a lack of standardized acquisition and analysis methods which could have led to unintended variability in the results. Finally, the variability in the timing of the acquisition of the post-gadolinium images could have influenced the enh measurement on static contrast-enhanced images; therefore our results may not be generalizable unless applied to static contrast-enhanced images performed 3 minutes after contrast administration (29).

Conclusions

Gadolinium-based contrast-enhanced rectal MRI using static T1-weighted imaging or quantitative DCE imaging may be a useful tool to predict pCR in mucinous rectal cancer, similar to non-mucinous tumors. Further work is warranted to tease out the post-neoadjuvant treatment enh and relative k_{ep} to get more granular results in larger populations before gadolinium contrast agent-based MRI can be applied clinically in the post-treatment distinction between residual tumor-containing mucin and acellular mucinous rectal tumors.

Acknowledgments

The authors thank Joanne Chin, MFA, ELS, for editing the manuscript.

Funding: This work was supported by a National Institutes of Health/National Cancer Institute Cancer Center Support Grant (No. P30 CA008748).

Footnote

Reporting Checklist: The authors have completed the STROBE reporting checklist. Available at https://qims.amegroups.com/article/view/10.21037/qims-23-1463/rc

Conflicts of Interest: All authors have completed the ICMJE uniform disclosure form (available at https://qims.amegroups.com/article/view/10.21037/qims-23-1463/coif). The authors have no conflicts of interest to declare.

Ethical Statement: The authors are accountable for all aspects of the work in ensuring that questions related to the accuracy or integrity of any part of the work are appropriately investigated and resolved. The study was conducted in accordance with the Declaration of Helsinki (as revised in 2013). The study was approved by the institutional review board of Memorial Sloan Kettering Cancer Center (IRB No. 18-136) and individual consent for this retrospective analysis was waived.

References

1. Bosman FT, Carneiro F, Hruban RH, Theise ND. WHO classification of tumours of the digestive system. No. Ed. 4.

World Health Organization, 2010.
2. Hugen N, van de Velde CJ, Bosch SL, Fütterer JJ, Elferink MA, Marijnen CA, Rutten HJ, de Wilt JH, Nagtegaal ID. Modern Treatment of Rectal Cancer Closes the Gap Between Common Adenocarcinoma and Mucinous Carcinoma. Ann Surg Oncol 2015;22:2669-76.
3. Mekenkamp LJ, Heesterbeek KJ, Koopman M, Tol J, Teerenstra S, Venderbosch S, Punt CJ, Nagtegaal ID. Mucinous adenocarcinomas: poor prognosis in metastatic colorectal cancer. Eur J Cancer 2012;48:501-9.
4. Barbaro B, Leccisotti L, Vecchio FM, Di Matteo M, Serra T, Salsano M, Poscia A, Coco C, Persiani R, Alfieri S, Gambacorta MA, Valentini V, Giordano A, Bonomo L. The potential predictive value of MRI and PET-CT in mucinous and nonmucinous rectal cancer to identify patients at high risk of metastatic disease. Br J Radiol 2017;90:20150836.
5. Wnorowski AM, Menias CO, Pickhardt PJ, Kim DH, Hara AK, Lubner MG. Mucin-Containing Rectal Carcinomas: Overview of Unique Clinical and Imaging Features. AJR Am J Roentgenol 2019;213:26-34.
6. McCawley N, Clancy C, O'Neill BD, Deasy J, McNamara DA, Burke JP. Mucinous Rectal Adenocarcinoma Is Associated with a Poor Response to Neoadjuvant Chemoradiotherapy: A Systematic Review and Meta-analysis. Dis Colon Rectum 2016;59:1200-8.
7. Kim MJ, Park JS, Park SI, Kim NK, Kim JH, Moon HJ, Park YN, Kim WH. Accuracy in differentiation of mucinous and nonmucinous rectal carcinoma on MR imaging. J Comput Assist Tomogr 2003;27:48-55.
8. Hussain SM, Outwater EK, Siegelman ES. Mucinous versus nonmucinous rectal carcinomas: differentiation with MR imaging. Radiology 1999;213:79-85.
9. Allen SD, Padhani AR, Dzik-Jurasz AS, Glynne-Jones R. Rectal carcinoma: MRI with histologic correlation before and after chemoradiation therapy. AJR Am J Roentgenol 2007;188:442-51.
10. Patel UB, Blomqvist LK, Taylor F, George C, Guthrie A, Bees N, Brown G. MRI after treatment of locally advanced rectal cancer: how to report tumor response--the MERCURY experience. AJR Am J Roentgenol 2012;199:W486-95.
11. Li SP, Padhani AR. Tumor response assessments with diffusion and perfusion MRI. J Magn Reson Imaging 2012;35:745-63.
12. Tofts PS. Modeling tracer kinetics in dynamic Gd-DTPA MR imaging. J Magn Reson Imaging 1997;7:91-101.
13. Tong T, Sun Y, Gollub MJ, Peng W, Cai S, Zhang Z, Gu Y. Dynamic contrast-enhanced MRI: Use in predicting pathological complete response to neoadjuvant chemoradiation in locally advanced rectal cancer. J Magn Reson Imaging 2015;42:673-80.
14. Intven M, Reerink O, Philippens ME. Dynamic contrast enhanced MR imaging for rectal cancer response assessment after neo-adjuvant chemoradiation. J Magn Reson Imaging 2015;41:1646-53.
15. Gollub MJ, Tong T, Weiser M, Zheng J, Gonen M, Zakian KL. Limited accuracy of DCE-MRI in identification of pathological complete responders after chemoradiotherapy treatment for rectal cancer. Eur Radiol 2017;27:1605-12.
16. Kim SH, Lee JM, Gupta SN, Han JK, Choi BI. Dynamic contrast-enhanced MRI to evaluate the therapeutic response to neoadjuvant chemoradiation therapy in locally advanced rectal cancer. J Magn Reson Imaging 2014;40:730-7.
17. George ML, Dzik-Jurasz AS, Padhani AR, Brown G, Tait DM, Eccles SA, Swift RI. Non-invasive methods of assessing angiogenesis and their value in predicting response to treatment in colorectal cancer. Br J Surg 2001;88:1628-36.
18. Lim JS, Kim D, Baek SE, Myoung S, Choi J, Shin SJ, Kim MJ, Kim NK, Suh J, Kim KW, Keum KC. Perfusion MRI for the prediction of treatment response after preoperative chemoradiotherapy in locally advanced rectal cancer. Eur Radiol 2012;22:1693-700.
19. Hoffmann U, Brix G, Knopp MV, Hess T, Lorenz WJ. Pharmacokinetic mapping of the breast: a new method for dynamic MR mammography. Magn Reson Med 1995;33:506-14.
20. Oberholzer K, Menig M, Pohlmann A, Junginger T, Heintz A, Kreft A, Hansen T, Schneider A, Lollert A, Schmidberger H, Christoph D. Rectal cancer: assessment of response to neoadjuvant chemoradiation by dynamic contrast-enhanced MRI. J Magn Reson Imaging 2013;38:119-26.
21. Saranathan M, Rettmann DW, Hargreaves BA, Clarke SE, Vasanawala SS. DIfferential Subsampling with Cartesian Ordering (DISCO): a high spatio-temporal resolution Dixon imaging sequence for multiphasic contrast enhanced abdominal imaging. J Magn Reson Imaging 2012;35:1484-92.
22. Medved M, Karczmar G, Yang C, Dignam J, Gajewski TF, Kindler H, Vokes E, MacEneany P, Mitchell MT, Stadler WM. Semiquantitative analysis of dynamic contrast enhanced MRI in cancer patients: Variability and changes in tumor tissue over time. J Magn Reson Imaging

2004;20:122-8.
23. Shen Y, Goerner FL, Snyder C, Morelli JN, Hao D, Hu D, Li X, Runge VM. T1 relaxivities of gadolinium-based magnetic resonance contrast agents in human whole blood at 1.5, 3, and 7 T. Invest Radiol 2015;50:330-8.
24. Li J, Gao X, Dominik Nickel M, Cheng J, Zhu J. Native T1 mapping for differentiating the histopathologic type, grade, and stage of rectal adenocarcinoma: a pilot study. Cancer Imaging 2022;22:30.
25. Parker GJ, Roberts C, Macdonald A, Buonaccorsi GA, Cheung S, Buckley DL, Jackson A, Watson Y, Davies K, Jayson GC. Experimentally-derived functional form for a population-averaged high-temporal-resolution arterial input function for dynamic contrast-enhanced MRI. Magn Reson Med 2006;56:993-1000.
26. Shia J, Guillem JG, Moore HG, Tickoo SK, Qin J, Ruo L, Suriawinata A, Paty PB, Minsky BD, Weiser MR, Temple LK, Wong WD, Klimstra DS. Patterns of morphologic alteration in residual rectal carcinoma following preoperative chemoradiation and their association with long-term outcome. Am J Surg Pathol 2004;28:215-23.
27. Cooper RA, Carrington BM, Loncaster JA, Todd SM, Davidson SE, Logue JP, Luthra AD, Jones AP, Stratford I, Hunter RD, West CM. Tumour oxygenation levels correlate with dynamic contrast-enhanced magnetic resonance imaging parameters in carcinoma of the cervix. Radiother Oncol 2000;57:53-9.
28. Dijkhoff RAP, Beets-Tan RGH, Lambregts DMJ, Beets GL, Maas M. Value of DCE-MRI for staging and response evaluation in rectal cancer: A systematic review. Eur J Radiol 2017;95:155-68.
29. Rieter JF, de Horatio LT, Nusman CM, Müller LS, Hemke R, Avenarius DF, van Rossum MA, Malattia C, Maas M, Rosendahl K. The many shades of enhancement: timing of post-gadolinium images strongly influences the scoring of juvenile idiopathic arthritis wrist involvement on MRI. Pediatr Radiol 2016;46:1562-7.

Cite this article as: El Homsi M, Yildirim O, Gangai N, Shia J, Gollub MJ, Mazaheri Y. Contrast-enhanced pelvic magnetic resonance imaging (MRI) for the prediction of treatment response in mucinous rectal cancer. Quant Imaging Med Surg 2024;14(6):4110-4122. doi: 10.21037/qims-23-1463

